Journal of Alloys and Compounds 520 (2012) 36–41

Contents lists available at SciVerse ScienceDirect

Journal of Alloys and Compounds

journal homepage: www.elsevier.com/locate/jallcom

Assessment of light scattering by pores in Nd:YAG transparent ceramics

Wei Zhang[a], Tiecheng Lu[a,b,*], Nian Wei[a], Yuezhong Wang[a], Benyuan Ma[a], Feng Li[a], Zhongwen Lu[a], Jianqi Qi[a]

[a] Department of Physics and Key Laboratory for Radiation Physics and Technology of Ministry of Education, Sichuan University, Chengdu 610064, PR China
[b] International Center for Material Physics, Chinese Academy of Sciences, Shenyang 110015, PR China

ARTICLE INFO

Article history:
Received 26 September 2011
Received in revised form 2 December 2011
Accepted 6 December 2011
Available online 16 December 2011

Keywords:
Nd:YAG
Transparent ceramics
Mie scattering theory
Scattering loss
Defects

ABSTRACT

Nd:YAG ceramic samples with different transmittances were fabricated by vacuum sintering with 10 °C/min or 2 °C/min heating rate. SEM measurements revealed that the average pore size of samples was around 0.18 μm while the porosity ranged from 0.0053% to 0.0022%. Mie scattering theory was applied to calculate the scattering coefficients as a function of the ratio between pore size and incident wavelength, pore size and porosity. The results showed that the simulated transmittances were in good agreement with the experimental values. The scattering loss was extremely low when the porosity was lower than 0.001% or the pore size was below 0.01 μm. A novel approach, to synergetically control the parameters of sizes and densities of the pores quantitatively for low scattering loss Nd:YAG ceramics, was presented. This quantitative insight into the pore scattering effects of Nd:YAG ceramics would allow a more targeted experimental optimization of this laser material.

1. Introduction

Transparent neodymium-doped yttrium aluminium garnet (Nd:YAG) crystals grown by the Czochralski method are widely used for solid-state laser gain media. Low duration and low cost of manufacturing, absence of severe limitation in size and geometry make the Nd:YAG ceramics attractive with comparison to single crystals [1–4]. Recently many advanced ceramic processing techniques have been explored to produce Nd:YAG ceramics, such as wet chemical method [5], slip-casting method [6], sintering additives [7,8].

Structural differences between single crystal and polycrystalline ceramics result in the existence of grain boundary and pores. Extensive studies about the fabrication of transparent ceramics largely concentrate on pores elimination and avoidance of second phases because they strongly cause light scattering. The relationship between the scattering loss and grain boundaries together with porosity were studied by Ikesue et al. [3,9]. They had investigated the influence of pores (with a porosity range of 0.015–0.093% and an average diameter of several micrometer) and grain boundary phase on scattering loss of Nd:YAG ceramics obtained by solid-state reaction method. It turned out that the effective scattering coefficients of Nd:YAG ceramics with pore volume of ~150 vol ppm were nearly equivalent to those of a 0.9 at.% Nd:YAG single crystal by Czochralski method. Boulesteix et al. demonstrated that the transparency and laser efficiency of Nd:YAG ceramics would be affected by the pores with a mean size of ~0.7 μm and concentration of 0.1–0.0001% [10]. Boulesteix et al. suggested that porosity should be less than 0.0001% to reach single-crystal laser efficiency with negligible scattering. Meanwhile, it is shown that, to obtain equivalent laser quality to single crystal, the Nd:YAG ceramics should be with low pore volume (~1 vol ppm) and narrow grain boundary (~1 nm) [2,11]. Additionally, Aschauer et al. showed that transparency of Nd:YAG ceramics was higher at smaller grain sizes [12]. On the other hand, Braun and Pilon suggested that the concentration of very small nanopores should have little effect on the scattering when the pore sizes are smaller than some certain value (which depends on the incident wavelength) [13]. Fedyk et al. revealed that light scattering of Nd:YAG nanoceramics strongly depended on the nano-pore size [14]. They pointed out that the decline of transmittance with decreasing wavelength observed in the Nd:YAG nanoceramics were induced by pores larger than 10 nm. A number of works have been done to investigate the influence of pores on the optical performance of transparent ceramics such as Al_2O_3 [15–18], Y_2O_3 [19] and yttria-stabilized ZrO_2 [20–23]. Our previous studies on nanometer polycrystalline $MgAl_2O_4$ showed that the nano-ceramics with porosity more than 1% could have high transparency (about 80%) [24,25]. The low or negligible light scattering mechanism was attributed to nano-sized pores and grains. We have also studied the influence of pore scattering on translucent AlON ceramics and advocated a new approach to control the sizes and densities of the pores for the

* Corresponding author at: Department of Physics and Key Laboratory for Radiation Physics and Technology of Ministry of Education, Sichuan University, Chengdu 610064, PR China. Tel.: +86 28 85412031; fax: +86 28 85412031.
E-mail addresses: lutiecheng@scu.edu.cn, qijianqi@cu.edu.cn (T. Lu).

0925-8388/$ – see front matter © 2011 Elsevier B.V. All rights reserved.
doi:10.1016/j.jallcom.2011.12.012

design of transparent ceramics [26]. In order to reduce the scattering loss of Nd:YAG ceramics, the porosity should be as small as possible. Unfortunately, it is impossible to eliminate the porosity completely in ceramics processing [16,22]. Therefore, a clearly theoretical assessment of light scattering as a function of pores should be highly desirable so as to optimize the manufacturing process, ultimately leading to better Nd:YAG laser ceramics.

In this study, transparent 2 at.% Nd:YAG ceramic samples were synthesized by vacuum sintering with the raw materials prepared by co-precipitation method. The light scattering loss of Nd:YAG ceramics in terms of pores was systematically investigated with the Mie scattering theory. The simulated results were presented along with experimental data. The aim of this present work was to assess the light scattering by pores in Nd:YAG ceramics and control the porosity level for low scattering loss Nd:YAG laser ceramics.

2. Experimental

The manufacturing process is similar to that reported in previous work [4]. Neodymium nitrate ($Nd(NO_3)_3{\cdot}6H_2O$, 99.99%), yttrium nitrate ($Y(NO_3)_3{\cdot}6H_2O$, 99.99%) and ammonium aluminum sulfate ($NH_4Al(SO_4)_2{\cdot}12H_2O$, 99.99%) were mixed together in stoichiometric proportions to form $Nd_{0.06}Y_{2.94}Al_5O_{12}$ (2 at.% Nd:YAG) in distilled water. The precipitant solution was prepared by dissolving ammonium hydrogen carbonate (NH_4HCO_3, analytical grade) in mixed solvent of alcohol and distilled water. The mixed solution was dripped into the precipitant solution at a dripping speed of 3 ml/min under stirring at 20 °C. With the suspension aged for 24 h, filtered and washed repeatedly with distilled water and alcohol in sequence, the precipitate was obtained. Then precursors were produced after the precipitate was dried at 80 °C for 24 h with an oven. The obtained precursors were calcinated at 1100 °C in order to produce the Nd:YAG nanopowders. The Nd:YAG nanopowders were blended with the high-purity Al_2O_3 balls for 24 h in ethanol using 0.5 wt.% tetraethylorthosilicate (TEOS) as a sintering aid. Then, the alcohol solvent was removed by drying the milled slurry in an oven, and residual organic material was removed by calcining at 800 °C for 20 h in flowing oxygen. The Nd:YAG nanopowders were uniaxially pressed into Ø 20 mm disks at 20 MPa and then isostatically cold pressed at 250 MPa. Then the compacted disks were sintered at 1780 °C for 20 h in a graphite-heated vacuum furnace under vacuum (1×10^{-3} Pa) with 10 °C/min or 2 °C/min heating rate. After cooling, the sintered samples were air annealed at 1450 °C for 20 h to eliminate oxygen vacancies formed during vacuum sintering. Thus, the samples were obtained and named as S1 (10 °C/min) and S2 (2 °C/min), respectively.

The phase structures of samples were identified by X-ray diffraction (XRD, Model D/max-rA, Rigaku, Japan). The samples were ground to a thickness of 2 mm and thoroughly polished carefully on both sides to eliminate surface scattering. The real in-line transmittances of samples were measured using an ultraviolet spectroscopy spectrometer (Spectrophotometer, Model UV-1700 Pharmaspec, Shimadzu, Japan) over the wavelength from 400 to 1100 nm. The distance between the sample and the detector was about 5.5 cm, and collection cone for the measurements was 0.5°. Scanning electron microscopy (SEM, Model S-4800, Hitachi, Japan) observations were conducted on thermally etched surface of samples to measure the size and volume of pores. The SEM images were taken at a magnification of 10,000 times for the samples unless the pores were too small to be detected. In order to determine pores quantitatively, we choose 25 images (each measurement Image 40 μm × 40 μm) that were located in an arrangement of a 5 × 5 lattice with an interval of 200 μm between each other in an area with a scale of 1000 μm × 1000 μm of every Nd:YAG specimen surface. Subsequently smaller images (5 μm × 5 μm) were taken over the pores one by one until all the pores in the larger scan were analyzed in every image. The apparent sizes of each pore in all images were manually defined by the MB-ruler software so that the area on the scale section could be counted.

3. Results and discussion

3.1. The phase structures and microstructure of Nd:YAG ceramic samples

Fig. 1 shows the XRD patterns of Nd:YAG ceramic samples with different heating rates. We can see that the phase structures of samples are almost the same despite of the different heating rates and introduction of neodymium and additives. All the diffraction peaks of the samples can be well indexed as the cubic garnet structure of $Y_3Al_5O_{12}$ (YAG, JCPDS 33-0040), and no other phases or impurities are detected.

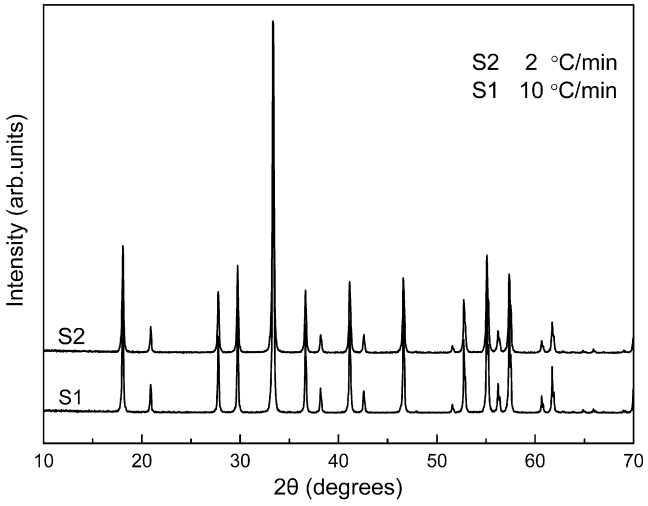

Fig. 1. XRD patterns of the Nd:YAG ceramic samples with heating rate: 10 °C/min (S1) and 2 °C/min (S2).

Fig. 2(a) shows a photograph of the mirror polished Nd:YAG ceramic samples sintered at 1780 °C for 20 h after annealing at 1450 °C for 20 h. Both samples are transparent, and the sample with heating rates of 2 °C/min exhibits a better transparency than the sample with heating rates of 10 °C/min. The transmittance

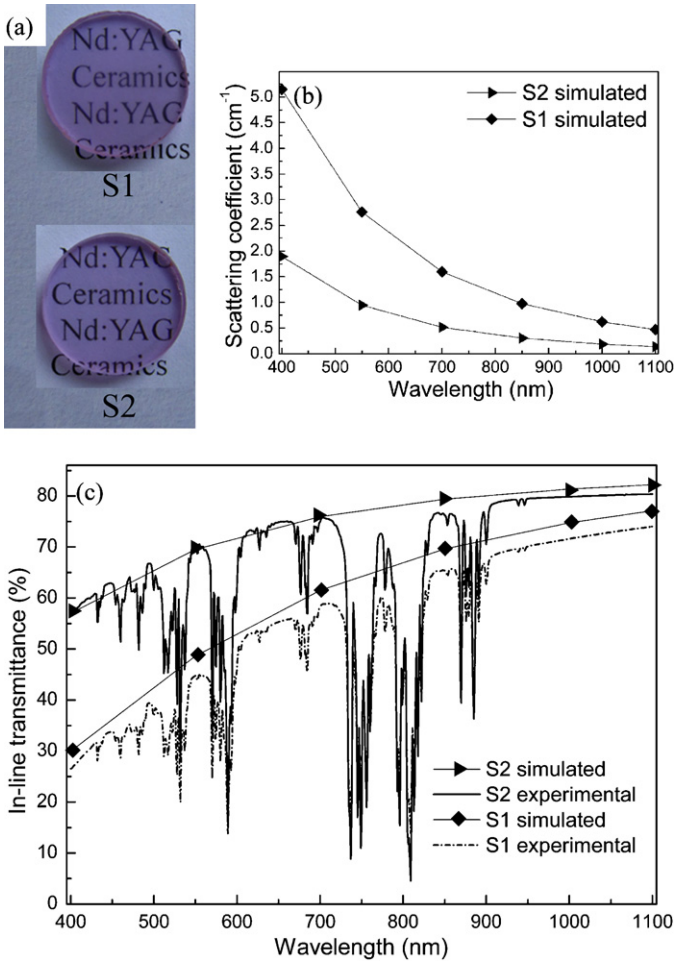

Fig. 2. (a) Photograph of the mirror polished Nd:YAG ceramic samples with heating rate: 10 °C/min (S1) and 2 °C/min (S2), (b) simulated scattering coefficients and (c) simulated and experimental in-line transmittances.

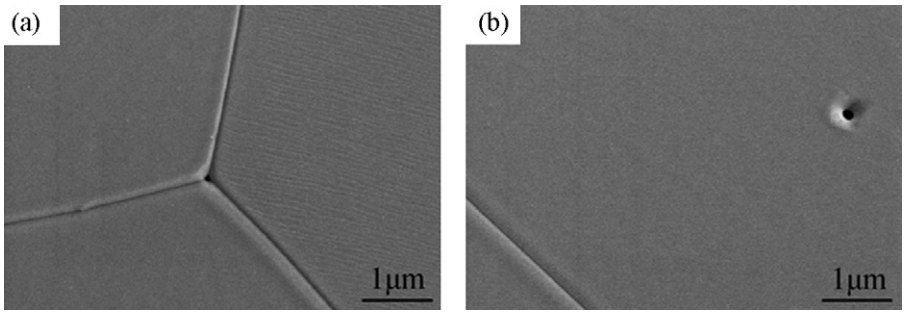

Fig. 3. The thermally etched surface of the sample (S1) with the heating rate of 10 °C/min: (a) the pore at the triple points of the grains and (b) the pore within the grain.

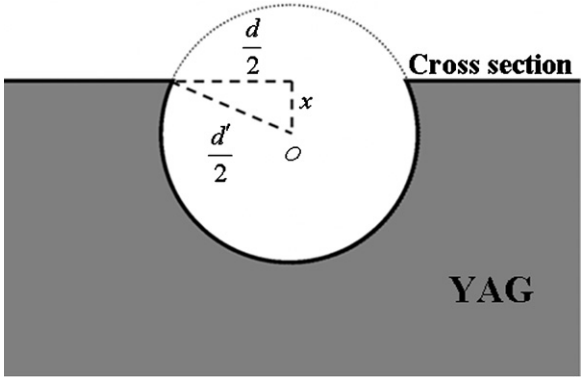

Fig. 4. Illustration of the pore intercepted by the thermally etched surface in YAG matrix.

increases drastically with the decrease of the heating rate, corresponding to the in-line transmittances shown in Fig. 2(b). The result indicates that the lower heating rate is beneficial to improve the optical properties of Nd:YAG ceramics.

In Fig. 3, we show images obtained from SEM for the sample with the heating rate of 10 °C/min. No other phases but a few submicrometer pores can be detected at the triple points of the grains or within the grains. As illustrated schematically in Fig. 4, d and d' are the apparent size and real size, respectively. We can approximate that x (the vertical distance between the pore centre and the cross section) is distributed randomly by considering large amount of pores. Then the average pore size (d') is obtained via Eqs. (1) and (2), by introducing a modified factor of 1.273 to the average apparent size (d) of the pores.

$$d = \frac{1}{d'} \int_{-d'/2}^{d'/2} \sqrt{(d'/2)^2 - x^2}\, dx = \frac{\pi}{4} d' \tag{1}$$

$$d' = \frac{4}{\pi} d \approx 1.273 d \tag{2}$$

Consequently, residual porosity V_p can be approximately acquired by counting the number of pores (N) in 25 images (S) by using Eq. (3).

$$V_P = \frac{N(\pi/6)d'^3}{S \cdot d'} = \frac{\pi N d'^2}{6S} \tag{3}$$

The results of the average pore sizes and concentrations of the samples are listed in Table 1 for further calculations.

From the data presented in Table 1, we note that the volume fraction of pores of Nd:YAG samples ranges from 0.0053% to 0.0022% while the sintering time at 1780 °C varied between 10 °C/min and 2 °C/min heating rate, respectively. The pores are formed in grain growth process during sintering while pore number decreases with decreasing heating rate. It is evident that pores are the primary scattering centres and increment in pore number is responsible for the transmission decrease.

3.2. The scattering coefficients and in-line transmittances

Since Nd:YAG is a cubic structure with no birefringence, pores and second phases are considered as the main scattering origins. Light scattering should be only due to the presence of residual pores evidenced by above phase structures and microstructure characterizations. The size of pores is submicrometer which is comparable to incident wavelength, so Mie scattering can occur. Mie scattering theory is applied on the assumption that the pores are approximated by spheres and are randomly dispersed in the ceramic matrix. Multiple scattering is not taken into account.

In presence of light scattering, the real in-line transmission can be expressed by the Lambert–Beer equation:

$$T(\lambda) = (1 - R_s) \cdot \exp(-C_{sca} \cdot t) \tag{4}$$

Here t is the sample thickness, C_{sca} is the effective scattering coefficient, and R_s is the fraction of light reflected at the surface as defined by the perpendicular total Fresnel reflectance:

$$R_s = \frac{2R'}{1 + R'}, \quad R' = \frac{(n-1)^2}{(n+1)^2} \tag{5}$$

The effective scattering coefficient of the pores can be expressed as follows:

$$C_{sca} = N_p \cdot G_P \cdot Q_{sca} = \frac{3V_p}{2d} Q_{sca} \tag{6}$$

Here N_p is the pore density, G_p is the geometrical cross section of the pores, d is the diameter of pores, V_p is the porosity of residual pores, and Q_{sca} is the scattering efficiency which can be calculated numerically using Mie scattering theory.

The refractive indexes of the samples (n) are from published results [27–29], and that of residual pores is set to 1. The intrinsic light absorption of Nd:YAG can be neglected at the wavelength 400, 550, 700, 850, 1000 and 1100 nm. Using the strict Mie theory [30,31], it is possible to calculate scattering coefficient values C_{sca}, for incident wavelengths at 400, 550, 700, 850, 1000 and

Table 1
The statistic data of the pore sizes and porosities in the samples.

Sample	Heating rate (°C/min)	Apparent pore size d (μm)	Pore size d' (μm)	Porosity V_p (%)
S1	10	0.1437	0.183	0.0053
S2	2	0.1225	0.156	0.0022

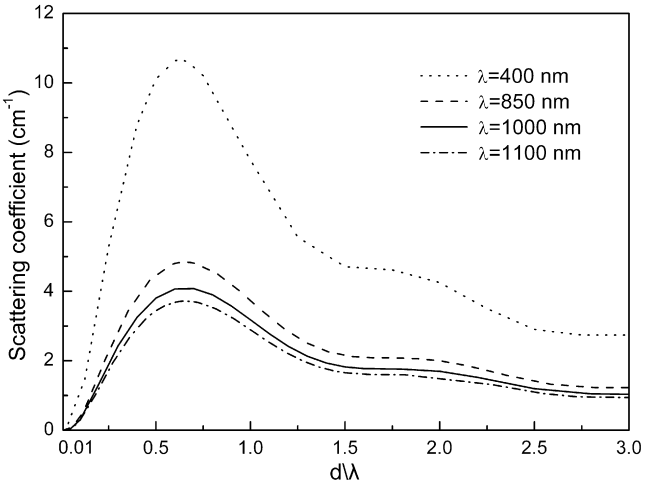

Fig. 5. Simulated scattering coefficients for Nd:YAG as a function of the ratio between pore size and incident wavelength, where d = 0.004–3.3 μm, λ = 400, 850, 1000 and 1100 nm, and porosity V_p = 0.01%.

1100 nm, when pores have average diameters fixed at 0.156 μm and 0.183 μm, respectively. The results of our Mie simulations using a dedicated computer program [32] are shown in Fig. 2(b) based on statistical data in Table 1. Note that the scattering coefficient of the sample with heating rates of 10 °C/min is much larger than that of the sample with heating rates of 2 °C/min and the scattering coefficient of pores gradually decreases with increasing wavelength. Using Eqs. (4) and (5), the transmittances of samples can be obtained, shown in Fig. 2(c). The experimental and simulated transmittances are in quite good agreement. Small statistical errors of pores and other defects caused by the existence of grain boundaries may explain the deviations of the simulations from experiments.

3.3. The effects of pore sizes and porosities on the light scattering of Nd:YAG ceramics

Even though there is a small amount of pores in our samples, it can result in significantly larger scattering loss than those of most previous published reports [2,3], as shown in Fig. 2(b). Hence it is very important to explore the influence on light scattering by pores in Nd:YAG ceramics. The light scattering, which is related to incident wavelength, pore size, and porosity, will be discussed in details.

To account for the effects of the relations between pore size and incident wavelength on scattering, the scattering coefficients as a function of the ratio between pore size and incident wavelength are shown in Fig. 5, where porosity V_p is 0.01%. For four different incident wavelengths λ = 400, 850, 1000 and 1100 nm, it is easily observed that the scattering coefficients increase with the ratio of d/λ in the beginning and then decrease when the ratio is close to 0.6–0.7. This tendency is attributed to the scattering coefficient C_{sca}, which is a function of the pore density N_p, the pore size d, and the scattering efficiency Q_{sca}, from Eq. (6). It is obvious that the maximum scattering coefficient values of all curves are at the ratio regions d/λ = 0.6–0.7. This indicates that the submicrometer pores as large as visible light wavelength can result in a strong scattering effect. A similar phenomenon was earlier reported in yttria-stabilized ZrO_2 ceramics [21]. Accordingly, we can conclude that the elimination of these submicrometer pores in ceramic manufacturing process has a significant effect on the reduction of scattering loss.

Fig. 6(a) shows the scattering coefficients as a function of porosity for different pore sizes d = 0.005–2 μm. For V_p = 0.0001–1%, the

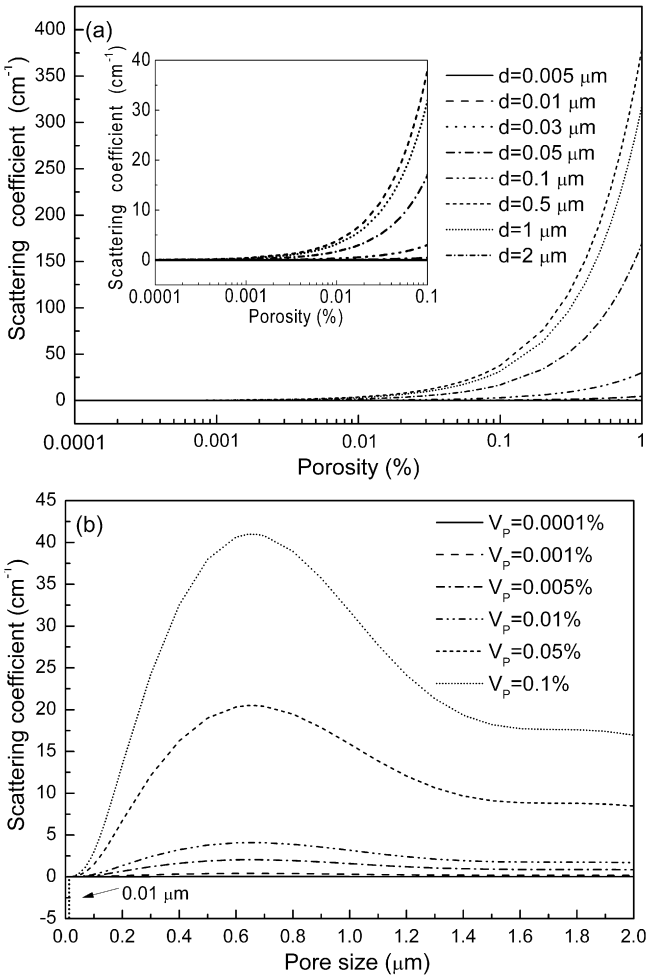

Fig. 6. (a) Simulated scattering coefficients as a function of porosity for different pore sizes, (b) simulated scattering coefficients as a function of pore size for different porosities, where d = 0.005–2 μm, porosity V_p = 0.0001–1%, incident wavelength λ = 1000 nm. *Inset*: simulated scattering coefficients as a function of porosity for different pore sizes, where porosity V_p = 0.0001–0.1%.

scattering coefficients drastically increase with porosity increased. As it is shown in inset of Fig. 6(a) the impact of porosity on scattering is extremely strong. Even at a porosity of only 0.01%, the scattering coefficients decrease from ~3.8 cm^{-1} to ~zero in this region of pore sizes. It is important to note that the pores can have little effect on light scattering when the porosity becomes lower than 0.001%.

Fig. 6(b) shows the scattering coefficients as a function of pore size for different porosities V_p = 0.0001%–1%. For the same pore size, the scattering coefficient C_{sca} simply increases with increasing porosity, whereas it increases in the beginning and then decreases with increasing pore radius, assuming the same porosity. Note that the scattering is very low for all porosities when the sizes are below 0.01 μm. Moreover, there is a significant increase when the pore size is larger than 0.01 μm. For d = 0.1 μm, the scattering coefficients decrease rapidly from ~3 to ~0.3 cm^{-1} with the porosity decreasing from 0.1% to 0.01%. Therefore, miniaturization and/or elimination of the residual pores are critical for promoting low scattering.

Just as many publications showing the 'critical size' related to the incident wavelength and porosity in other transparent ceramics [22,25], Fedyk et al. revealed that the scattering was negligible in Nd:YAG nanoceramics when pore size was <15 nm (at 500 nm incident light wavelength) or pore size was <35 nm (at 1100 nm incident light wavelength) [14]. However, Ikesue

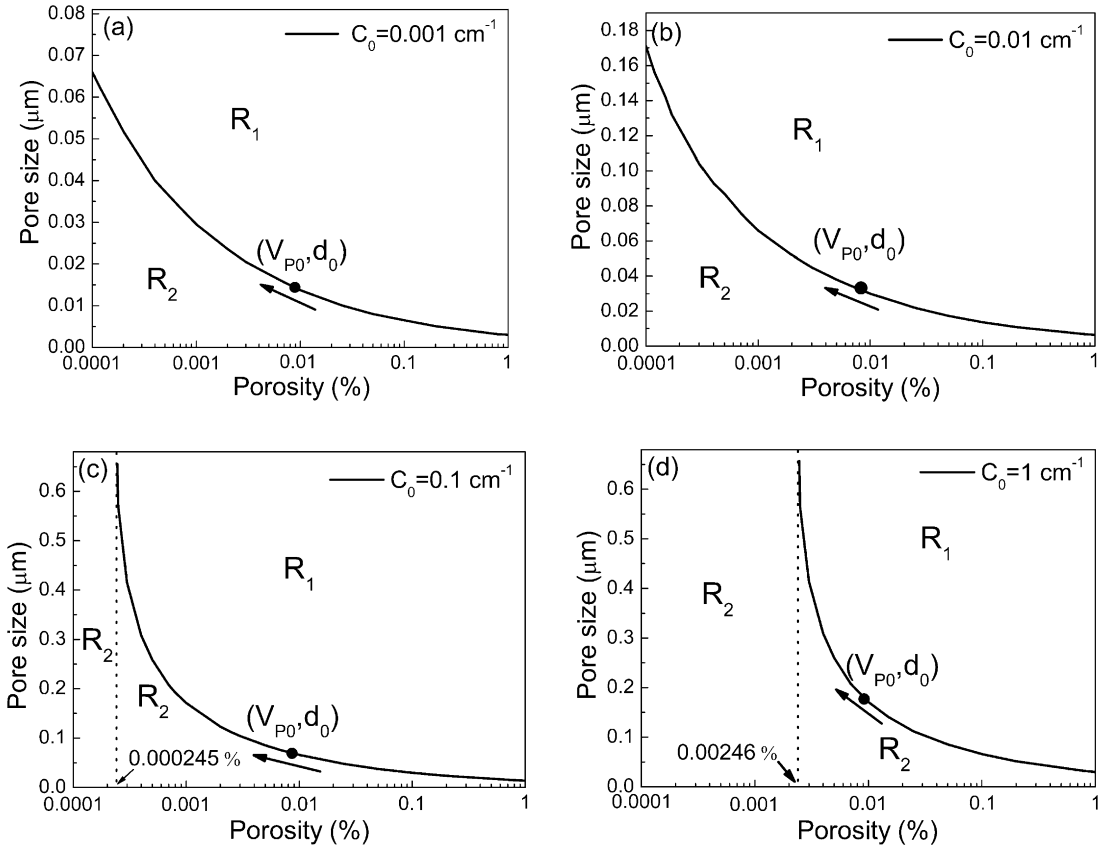

Fig. 7. The low scattering demarcation curves (a) $C_0 = 0.001\ cm^{-1}$, (b) $C_0 = 0.01\ cm^{-1}$, (c) $C_0 = 0.1\ cm^{-1}$ and (d) $C_0 = 1\ cm^{-1}$ of Nd:YAG ceramics at the incident wavelength of $\lambda = 1000$ nm. Region R_1 denotes $C_{sca} > C_0$ and R_2 shows $C_{sca} < C_0$. The dotted lines are asymptotes of the scattering demarcation curves.

et al. reckoned that the scattering can be neglected when below 150 ppm while other authors proposed that value under 1 ppm [2,9–11]. Meanwhile, from our analysis mentioned above, it has been suggested that the value of 0.001% for porosity and 0.01 μm for pore size are critical parameters of pores for Nd:YAG to achieve low scattering loss. These discrepancies of light scattering loss should have originated most probably from the differences of pore sizes and their concentrations. Yet a unified standard that can clearly evaluate scattering loss in term of the porosity level has not been developed. Here, we propose that the terms critical size/critical concentration of the pores should be reserved for the specific scattering loss with different porosities/average pore sizes and, respectively, the corresponding maximal tolerant limit of the average pore size/porosity. And the terms scattering demarcation curves of pores shown in Fig. 7, which were quantitatively characterized by critical size and critical concentration of pores, should be reserved for Nd:YAG ceramics with different scattering losses over the wavelengths of interest. According to previous experimental reports, the scattering loss of excellent quality transparent Nd:YAG ceramics with different thickness is between 0.002 and 0.009 cm^{-1} when incident wavelength is around 1000 nm, which is almost the same as that of single crystal [2,3]. In order to better understand this relationship, the different low scattering demarcation curves ($C_{sca} = 0.001–1\ cm^{-1}$) of Nd:YAG at the wavelength of 1000 nm as a function of porosities and pore sizes are shown in Fig. 7. It is to be noted that the low scattering demarcation curve is characterized by critical sizes, D_0 and critical concentrations, V_{P0}, which divide the scattering loss region into two parts: R_1 ($C_{sca} > C_0$) and R_2 ($C_{sca} < C_0$) depending on porosity and pore size. As shown in this figure, high critical concentration will sacrifice the critical size and vice versa in every curve. It is interesting to note that the critical size/critical concentration of different low demarcation curves increases with the scattering coefficient increasing from 0.001 to 1 cm^{-1}. In Fig. 7(a), the critical size varies from ~0.003 to ~0.066 μm at the scattering coefficient of 0.001 cm^{-1} while critical concentration ranges from 0.0001% to 1%. In Fig. 7(b), the critical size varies from ~0.006 to ~0.17 μm at the scattering coefficient of 0.01 cm^{-1} while critical concentration ranging from 0.0001% to 1%. In Fig. 7(c), the critical size varies from ~0.014 to ~0.66 μm at the scattering coefficient of 0.1 cm^{-1} while critical concentration ranges from 0.000245% to 1%, and the scattering coefficient falls into the region of R_2 (which means $C_{sca} < C_0$) whatever the value of pore size in the region as long as the critical concentration is <0.000245%. In Fig. 7(d), the critical size varies from ~0.03 to ~0.66 μm at the scattering coefficient of 1 cm^{-1} while critical concentration ranges from 0.00246% to 1%, and the scattering coefficient falls into the region of R_2 (which means $C_{sca} < C_0$) whatever the value of pore size in the region as long as the critical concentration is <0.00246%. Consequently, the different low scattering losses can be achieved by synergetic controlling the parameters of the pores to get across the scattering demarcation curve from porosity region R_1 to enter into R_2. On the contrary, if we have obtained the scattering loss value of Nd:YAG ceramic sample, we can speculate its porosity level on the basis of the scattering demarcation curves. Obviously, the result is equally applicable to Nd:YAG ceramics with different thickness as well as similar to those of other wavelengths. So here a novel approach which is used to guide synergetic controlling the pore sizes and porosities quantitatively for low scattering loss Nd:YAG ceramics is presented.

Pore-free ceramics with nanosized grains may display new optical, mechanical, electrical or other properties with great potential for applications [33]. Recently many interesting studies have

concerned structural and optical properties of Nd:YAG nanoceramics [14,34–36] but no successful laser oscillation has been reported so far. This should be the result of light scattering by high nanosized pores content in nanoceramics. It is generally accepted that Mie theory can be extended very effectively to explain the optical properties of homogeneous particles sizes in the nanometer, submicrometer and micrometer range. Given the interest in the low scattering loss of the laser material, the analysis of such low scattering demarcation curves should provide guidance on the fabrication of Nd:YAG ceramics of nanosized and microsized grains.

4. Conclusions

We have investigated the influence of pores on the light scattering of Nd:YAG ceramic samples based on the Mie scattering theory and the statistical results of pores. The scattering coefficients are simulated as a function of the ratio between pore size and incident wavelength, pore size and porosity. The results show that the simulated transmittances from the model agree well with the experimental data. The submicrometer pores which are as large as visible light wavelength can give rise to a strong scattering effect. The scattering is extremely low when the porosity is lower than 0.001% or the pore size is below 0.01 μm. Miniaturization and/or elimination of the pores are critical for promoting low scattering loss. Additionally, low scattering loss (C_{sca} = 0.001–0.01 cm^{-1}) for Nd:YAG can be achieved by carefully synergetic controlling pore sizes and porosities to get across the low scattering demarcation curves and enter the region R_2, as quantitatively presented in this paper. The present work should allow a more fundamental understanding of the pore scattering effects of Nd:YAG ceramics and probably provide guidance on the fabrication of Nd:YAG ceramics of nanosized and microsized grains.

Acknowledgements

This work was supported by the National Natural Science Foundation of the People's Republic of China (Grant Nos. 50872083 and 51002098), the Doctoral Program of Higher Education (Grant No. 20090181120092) and the National High Technology Research and Development Program (863).

References

[1] A. Ikesue, Y.A. Aung, Nat. Photon. 2 (12) (2008) 721–727.
[2] J. Lu, M. Prabhu, J. Xu, K.I. Ueda, H. Yagi, T. Yanagitani, A.A. Kaminskii, Appl. Phys. Lett. 77 (2003) 707–709.
[3] A. Ikesue, K. Yoshida, T. Yamamoto, I. Yamaga, J. Am. Ceram. Soc. 80 (6) (1997) 1517–1522.
[4] W. Zhang, T.C. Lu, N. Wei, B.Y. Ma, F. Li, Z.W. Lu, J.Q. Qi, Opt. Mater. (2011), doi:10.1016/j.optmat.2011.10.001.
[5] Y.H. Sang, H. Liu, X.D. Sun, X.L. Zhang, H.M. Qin, Y.H. Lv, D. Huo, D. Liu, J.Y. Wang, R.I. Boughton, J. Alloys Compd. 509 (2011) 2407–2413.
[6] Y.H. Lv, W. Zhang, J. Tan, Y.H. Sang, H.M. Qin, J.L. Hua, L.N. Tong, H. Liu, J.Y. Wang, R.I. Boughton, J. Alloys Compd. 509 (2011) 3122–3127.
[7] Y.K. Li, S.M. Zhou, H. Lin, X.R. Hou, W.J. Li, H. Teng, T.T. Jia, J. Alloys Compd. 502 (2010) 225–230.
[8] H. Yang, X.P. Qin, J. Zhang, S.W. Wang, J. Ma, L.X. Wang, Q.T. Zhang, J. Alloys Compd. 509 (2011) 5274–5279.
[9] A. Ikesue, K. Yoshida, J. Mater. Sci. 34 (1999) 1189–1195.
[10] R. Boulesteix, A. Maître, J.-F. Baumard, Y. Rabinovitch, F. Reynaud, Opt. Exp. 18 (2010) 14992–15002.
[11] G.A. Kumar, J. Lu, A.A. Kaminskii, K.-I. Ueda, H. Yagi, T. Yanagitani, IEEE J. Quantum Electron. 40 (6) (2004) 747–758.
[12] U. Aschauer, P. Bowen, J. Am. Ceram. Soc. 93 (3) (2010) 814–820.
[13] M.M. Braun, L. Pilon, Thin Solid Films 496 (2006) 505–514.
[14] R. Fedyk, D. Hreniak, W. Łojkowski, W. Stręk, H. Matysiak, E. Grzanka, S. Gierlotka, P. Mazur, Opt. Mater. 29 (2007) 1252–1257.
[15] R. Apetz, M.P.B. van Bruggen, J. Am. Ceram. Soc. 86 (3) (2003) 480–486.
[16] A. Krell, T. Hutzler, J. Klimke, J. Eur. Ceram. Soc. 29 (2) (2009) 207–221.
[17] B. Kim, K. Hiraga, K. Morita, H. Yoshida, T. Miyazaki, Y. Kagawa, Acta Mater. 57 (5) (2009) 1319–1326.
[18] B.N. Kim, K. Hiraga, K. Morita, H. Yoshida, Y. Kagawa, Acta Mater. 58 (2010) 4527–4535.
[19] C. Greskovich, J.P. Chernoch, J. Appl. Phys. 44 (1973) 4599–4606.
[20] U. Anselmi-Tamburini, J.N. Woolman, Z.A. Munir, Adv. Funct. Mater. 17 (2007) 3267–3273.
[21] K. Tsukuma, I. Yamashita, T. Kusunose, J. Am. Ceram. Soc. 91 (3) (2008) 813–818.
[22] A. Krell, J. Klimke, T. Hutzler, Opt. Mater. 31 (2009) 1144–1150.
[23] H.B. Zhang, B.N. Kim, K. Morita, H. Yoshida, J.H. Lim, K. Hiraga, J. Am. Ceram. Soc. 94 (9) (2011) 2981–2986.
[24] T.C. Lu, X.H. Chang, J.Q. Qi, X.J. Luo, Q.M. Wei, S. Zhu, K. Sun, J. Lian, L.M. Wang, Appl. Phys. Lett. 88 (2006) 213120.
[25] J. Zhang, T.C. Lu, X.H. Chang, N. Wei, W. Xu, J. Phys. D: Appl. Phys. 42 (2009) 052002.
[26] Y.Z. Wang, T.C. Lu, L. Gong, J.Q. Qi, J.S. Wen, J. Yu, L. Pan, Y. Yu, N. Wei, J. Phys. D: Appl. Phys. 43 (2010) 275403.
[27] W.L. Bond, J. Appl. Phys. 36 (5) (1965) 164–167.
[28] M. Sekita, H. Haneda, S. Shirasaki, T. Yanagitani, J. Appl. Phys. 69 (6) (1991) 3709–3718.
[29] E.D. Palik (Ed.), Handbook of Optical Constants of Solids, vol. 3, Academic Press, New York, 1991, p. 976.
[30] H.C. van de Hulst, Light Scattering by Small Particles, Dover, New York, 1982, pp 119–130.
[31] C.F. Bohren, D.R. Huffman, Absorption and Scattering of Light by Small Particle, Wiley, New York, 1983.
[32] M. Bernhard, http://omlc.ogi.edu/calc/mie calc.html.
[33] G.L. Messing, A.J. Stevenson, Science 332 (17) (2008) 383–384.
[34] D. Hreniak, W. Strek, J. Alloys Compd. 341 (2002) 183–186.
[35] D. Hreniak, R. Fedyk, A. Bednarkiewicz, W. Stręk, W. Łojkowski, Opt. Mater. 29 (2007) 1244–1251.
[36] D. Hreniak, W. Strek, P. Głuchowski, R. Fedyk, W. Łojkowski, J. Alloys Compd. 451 (2008) 549–552.